

# Finite Element Simulation of Multi-Stage Deep Drawing Processes & Comparison with Experimental Results

A. Pourkamali Anaraki, M. Shahabizadeh, and B. Babae

**Abstract**—The plastic forming process of sheet plate takes an important place in forming metals. The traditional techniques of tool design for sheet forming operations used in industry are experimental and expensive methods. Prediction of the forming results, determination of the punching force, blank holder forces and the thickness distribution of the sheet metal will decrease the production cost and time of the material to be formed. In this paper, multi-stage deep drawing simulation of an Industrial Part has been presented with finite element method. The entire production steps with additional operations such as intermediate annealing and springback has been simulated by ABAQUS software under axisymmetric conditions. The simulation results such as sheet thickness distribution, Punch force and residual stresses have been extracted in any stages and sheet thickness distribution was compared with experimental results. It was found through comparison of results, the FE model have proven to be in close agreement with those of experiment.

**Keywords**—Deep drawing, Finite element method, Simulation.

## I. INTRODUCTION

A commonly used sheet metal forming process is deep drawing process. In this process, hollow products are produced in 1-step drawing or multi-step drawing. Multi-step drawing processes are usually applied to forming parts that have geometrical complexity or formability problems and cannot be formed by 1-step forming. In these cases, one of the most critical and challenging issues is to determine minimum required forming steps and the corresponding part shapes in any forming steps [1].

Traditional design methods for sheet metal forming are usually based on a trial-and-error or empirical approach. Recently, due to the demand of high precision and reliability in formed metal parts, these methods are difficult and sometimes handicapped to provide a solution.

A. Pourkamali Anaraki, Department of Mechanical Engineering, Langaroud Branch, Islamic Azad University, Langaroud, Iran (phone: +98-9121136927; e-mail: ali\_pourkamali@iaul.ac.ir).

M. Shahabizadeh is with the Mechanical Engineering Department, Shahid Rajaei Teacher Training University, Tehran, Iran (phone: +98-021-22970025; e-mail: hannyshahabi@yahoo.com).

B. Babae was with the Mechanical Engineering Department, Shahid Rajaei Teacher Training University, Tehran, Iran (phone: +98-021-22970060; e-mail: babae1386@gmail.com).

Finite element method (*FEM*) is being gradually adopted by industry to predict the formability of sheet metals.

Sheet metal forming operation involves complex physical mechanisms that give rise to a high order non-linear problem. Apart from the nonlinearity induced by the contact and the friction, there is a geometrical non-linearity caused by large displacement and large deformation. Furthermore, non-linear material behaviors such as plasticity make the problem even more difficult to be solved analytically. Therefore, numerical techniques, such as FEM, are usually used to deal with this kind of problem. FEM can provide not only the final results, but also the information of intermediate steps, like the distributions of displacement, stress, strain and other internal variables [2].

Single-stage deep drawing simulation has been investigated by many of researchers, but in multi-stage deep drawing it has been less than to be attended. However, a number of difficulties have been encountered because of strong non-linearity and then element re-meshing technique is required to eliminate severe element distortions. Some of the researchers amongst, Min et al [3], Kim et al [4], Ku et al [5], Fan et al [6] and Kim et al [2] studied in this case. This paper is also considering to simulation of multi-stage deep drawing of an Industrial Part by 2D-axisymmetric models in ABAQUS software and then comparison with experimental results.

## II. INDUSTRIAL PART DESCRIPTION

Production process of an industrial part with its dimensions is shown in Fig. 1. Material of used sheet is aluminum alloy 7075-O.

AA7075-O is one of the high strength aluminum alloys and is very difficult to be formed by deep drawing process. Mechanical properties of sheet are presented in Table I.

Multi-stage deep drawing simulation of industrial part is performed on basis of experimental die dimensions and is discussed in next section.

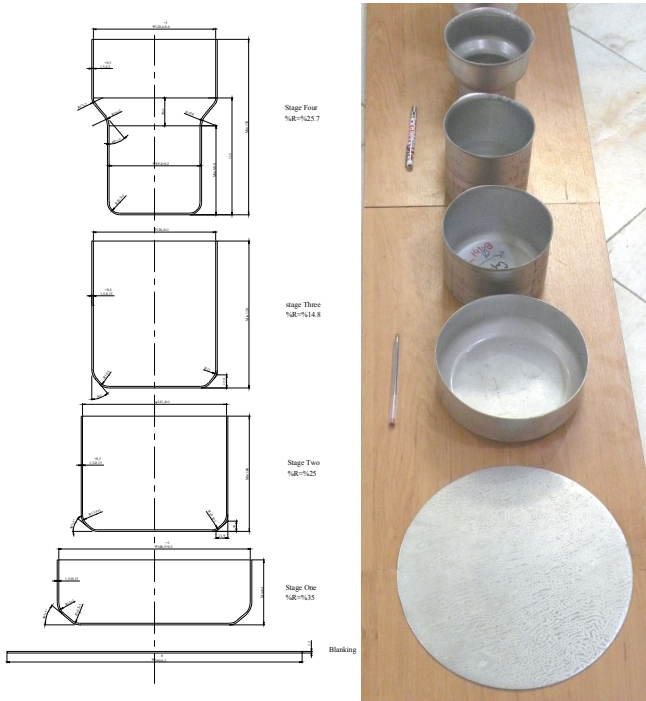


Fig. 1 Production process of industrial part with its dimensions

TABLE I  
 MECHANICAL PROPERTIES OF 7075-O ALUMINUM ALLOY [7]

Symbol	Parameter	Value
$\rho$	Density	2800 Kg/m <sup>3</sup>
$S_u$	Ultimate tensile strength	248.4 Mpa
$S_y$	Yield strength	138 Mpa
$E$	Module of elasticity	71.7 Gpa
$\nu$	Poisson ratio	0.33
%EL	Elongation in 50 mm ( 2 inch )	10%
HB	Brinell hardness	60

### III. FINITE ELEMENT SIMULATION

Finite element simulation of multi-stage deep drawing is performed in ABAQUS software, version 6-9-1. Analysis of the drawing process is based on the axisymmetric condition. Hence, only the right half of the tools such as punch, die and blank holder is modeled according Fig. 2.

The continuum or solid elements, the shell elements and the membrane elements are three main types of finite elements that can be used in the computer modeling of the blank and tooling elements, and various references may be cited in the development of element formulations capable of modeling large deformation kinematics in the total, updated or co-rotational sense for these finite element types [8].

The finite element meshes of the forming tools are usually intended to impose the forming loads to the sheet metal through the forming interface. Because of the fact that the forming tools should be, theoretically, designed to be rigid and the die-face deformations should be elastic with minimal shape changes, Hence, tools deformations are negligible and have been modeled as discrete rigid parts and only the surface geometry of the forming tools are included in simulation

models. Also, sheet is modeled as deformable shell. Entire modeling data is taken from designed dies dimensions and has presented in Table II. Mechanical properties of sheet are introduced to software from Table I and Fig. 3.

Since, majority of metal forming processes are quasi-static problems, therefore, Dynamic Explicit method is suitable for these types of problems. Penalty function method was used to treat the contact algorithm. The friction coefficient between the punch and sheet was assumed 0.2 and sheet with die and blank holder was 0.1. Moreover, to prevent wrinkling in the sheet drawing process, a blank holder pressure up to 15 bars, during the forming process was applied over blank holders for each case. For meshing of tools (punch, die and blank holder), 2-node linear axisymmetric rigid link elements (RAX2) were used. Because of the ironing process was occurred in end of drawing, Shell elements or Membrane elements were not suit for meshing of sheet and have been gave illusive results. Hence, 4-node bilinear axisymmetric quadrilateral solid element with reduced integration (CAX4R) was used for meshing of deformable sheet. On the other hand, central area of blank was not critical in deep drawing analysis; therefore meshing size in central section of blank was greater than other sections to reaching the less time for analysis. Sheet meshing is illustrated in Fig. 4.

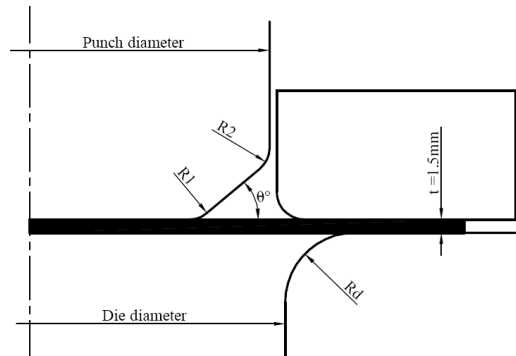


Fig. 2 The general geometry of sheet and tools used in simulation

TABLE II  
 BLANK, DIE AND PUNCH DIMENSIONS IN VARIOUS STEPS

Parameter	Step-1	Step-2	Step-3	Step-4
Punch diameter (mm)	188.5	141.4	120.4	89.4
Die diameter (mm)	191.9	144.6	124	92.6
Punch edge radius (mm)	R <sub>1</sub> =10.5 R <sub>2</sub> =15	R <sub>1</sub> =10.5 R <sub>2</sub> =13.5	R <sub>1</sub> =10.5 R <sub>2</sub> =12	R <sub>p</sub> =10.5
Die edge radius (mm)	R <sub>d</sub> =10	R <sub>d1</sub> =12 R <sub>d2</sub> =16.5	R <sub>d1</sub> =12 R <sub>d2</sub> =15	R <sub>d1</sub> =18 R <sub>d2</sub> =18
Punch and Die edge chamfer (degree)	theta=40°	theta=40°	theta=40°	theta=40°
Blank diameter (mm)	290	-	-	-

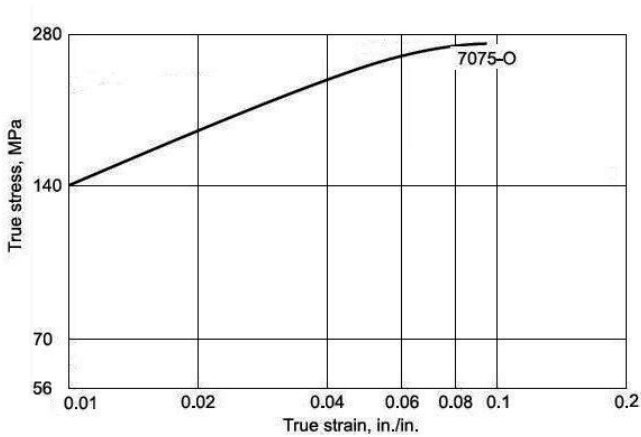


Fig. 3 Plasticity behavior of AA7075-O [9]



Fig. 4 The geometry of mesh for blank

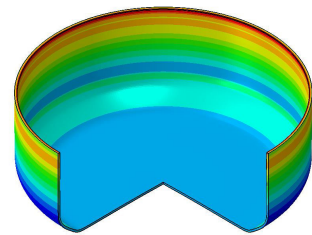
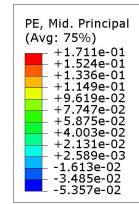
A deviating shape is caused by elastic springback after forming and retracting the tools. Therefore, the entire 4-step drawings have been solved including springback after each drawing step. Springback is simulated through an implicit calculation which is solved with the aid of ABAQUS Standard. The deformed shapes for each step and plastic strain values of them as color contours are shown in Fig. 5.

It is necessary to say the annealing operation was performed after second step, therefore to simulation of annealing operation in ABAQUS software, an orphan mesh was imported to third step from final drawn part in second step. This operation nullified stress and strain history.

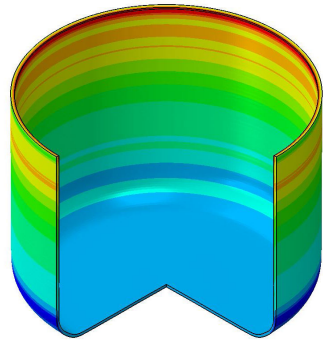
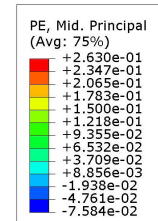
Experimental results are included thickness distribution of deformed parts in any steps, and have been extracted by measuring of wall thickness in various points on produced parts. These results has been presented in next section and then compared with FE simulation results.

#### IV. COMPARISON OF FINITE ELEMENT RESULTS WITH EXPERIMENTAL RESULTS

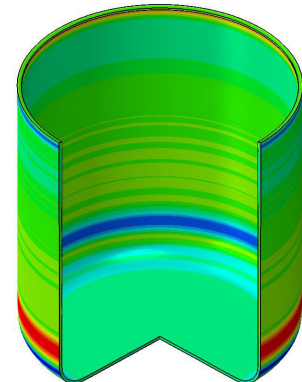
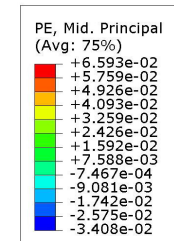
Figs. (6)-(9) provide a comparison of the sheet-thickness distribution after drawing for numerical simulations and for experiments. It is intelligible from comparing of simulated results with experimental data so that the FEM predicted trends for all of the cases are in good agreement with experimental data. However, in some of points such as punch corners have errors and these errors have been increased in third and fourth steps. It is because of changes in plastic behavior of initial sheet due to work hardening. This condition is not considered in simulation analysis. Therefore, errors are increased in these cases. Maximum error in this simulation is up to 10%.



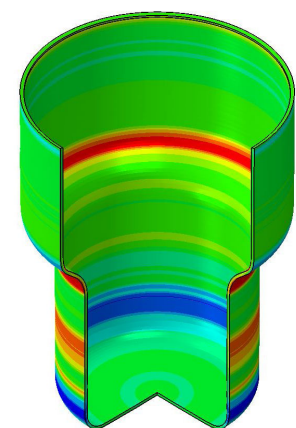
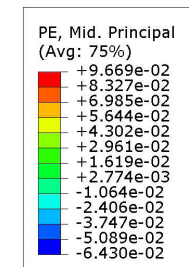
(a)



(b)



(c)



(d)

Fig. 5 Plastic strain values of deformed shapes for each step

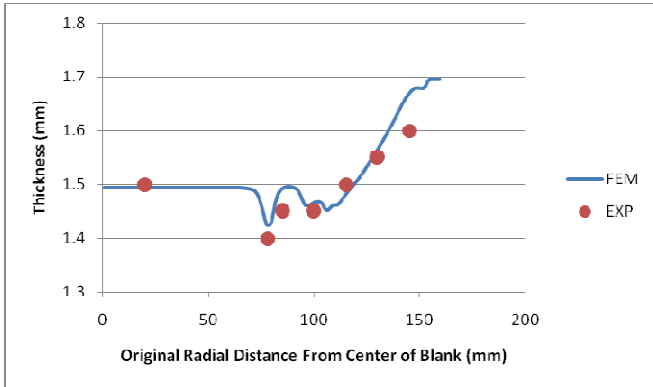


Fig. 6 Thickness distribution in step-1

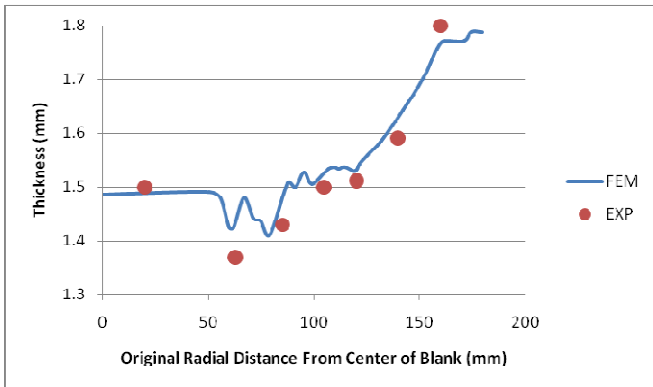


Fig. 7 Thickness distribution in step-2

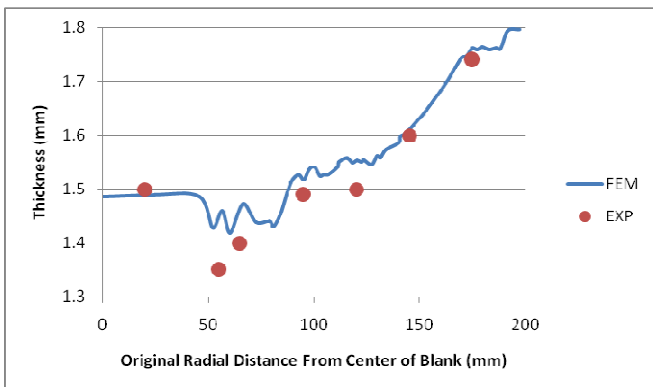


Fig. 8 Thickness distribution in step-3

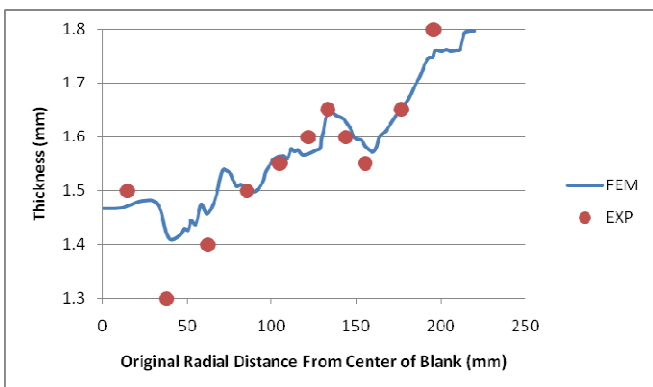


Fig. 9 Thickness distribution in step-4

The diagrams of sheet thickness distribution confirm the FE simulation is to be authentic. Therefore, other simulation results such as punch forces for any step have been extracted from finite element analysis. In Fig. 10 maximum punch force for any drawing steps has presented and compared with that from generally accepted formula for predicting maximum punch load at die design literatures [10].

It is seen from fig. 10, the punch force is higher in first step and decreased by going on subsequent steps so that it was expected from generally accepted formula for predicting maximum punch load. Punch force is in straight relation with punch diameter according to (1) [10]:

$$F_{punch} = S_u \times \pi \times d_{punch} \times t \quad (1)$$

According to (1), the higher diameter of punch, then higher punch force. Therefore, FEM results for punch load are in good agreement with (1) by about %25 differences between them.

Fig. 11 provides a comparison of the punch force variations versus punch stroke in various steps. These results have extracted from numerical simulation. It is seen from fig. 11, the punch force for stage-2 has increased at end of punch stroke. This demonstrates the deformed part in stage-2 is to be experiencing Ironing process at the end of punch stroke due to unsuitable clearance between punch and die.

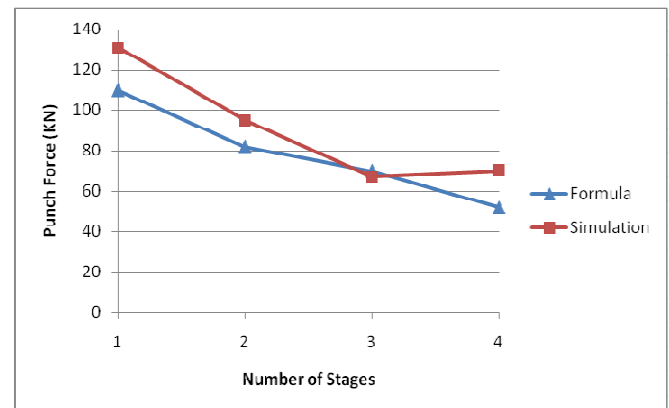


Fig. 10 Comparison of simulated and calculated punch forces

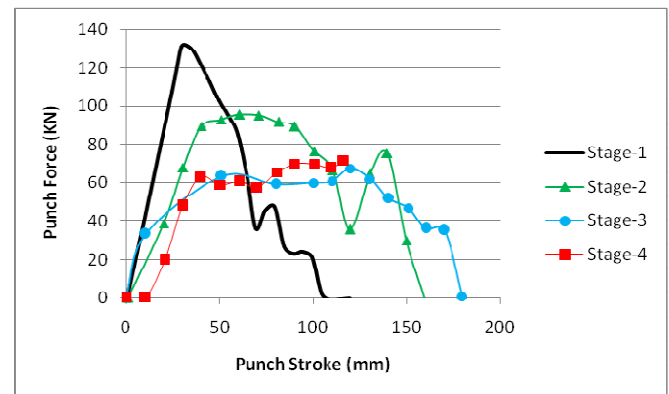


Fig. 11 Punch force versus punch stroke in various steps

Residual stresses at deformed parts in any steps have extracted from simulation analysis and are shown in Fig. 12. These results were expected, because the central area of blank was not critical in deep drawing analysis, therefore residual stress in central section of blank was less than other sections. On the other hand, the residual stresses are rising with proceeding in next stages. It is because of work hardening has been increased with next stages in deep drawing.

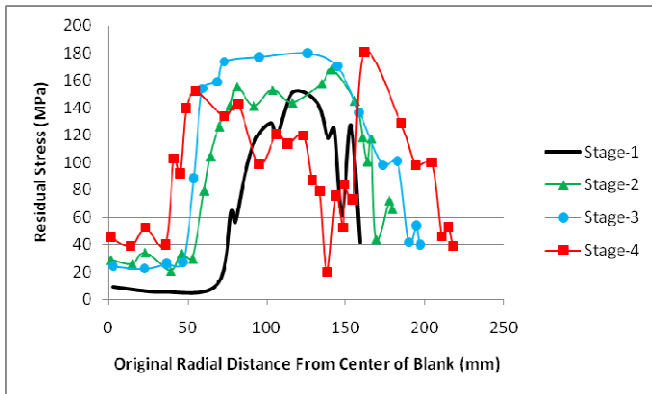


Fig. 12 Residual stress in various steps

#### V. CONCLUSION

Comparison of experimental and FEM simulation results on the multi-stage drawing process were performed in this study.

It was found through comparison of thickness distribution in produced parts with simulated deep drawing parts, the finite element model have proven to be in qualitative agreement with those of experiment in primary steps, but because of the changes in plastic behavior of initial sheet, errors were increased in last steps. Maximum errors in this simulation were up to 10% on the punch corners in fourth step. Therefore, it is necessary to reinvestigation on material properties after any steps and to applying these changes in next steps.

It was found through FE simulation, the punch force is higher in first stage and it is decreasing with proceeding in next stages. Predicted punch forces were in good agreement with calculated punch force from formula in die design literatures.

Residual stresses are lesser in central area of blank and those are rising with proceeding in next stages.

Finite element modeling (FEM) can accurately portray forming from a particular die design without the need for costly trial and error. With simulation via FEM, designers can estimate field variables such as strain distribution, stress distribution, material flow and forming defects. This information enhances the design capability and knowhow of an experienced process designer and leads to a reduced number of die-tryout tests.

#### REFERENCES

[1] J. Cao, Sh. Li, Z. C. Xia, S. C. Tang, 2001, "Analysis of an axisymmetric deep-drawn part forming using reduced forming steps", *Journal of Material Processing Technology*. Vol 117, pp. 193–200.

[2] H. K. Kim, S. K. Hong, 2007, "FEM-based optimum design of multi-stage deep drawing process of molybdenum sheet", *Journal of Material Processing Technology*. Vol 184, pp. 354–362.

[3] D.K. Min, B.H. Jeon, H.J. Kim, N. Kim, 1995, "A study on process improvements of multi-stage deep-drawing by the finite-element method", *J. Mater. Process. Technol.* Vol 54, pp. 230–238.

[4] S. H. Kim, S. H. Kim, H. Huh, 2002, "Tool design in a multi-stage drawing and ironing process of a rectangular cup with a large aspect ratio using finite element analysis", *Int. J. Mach. Tool Manuf.* Vol 42, pp. 863–875.

[5] T. W. Ku, B. K. Ha, W. J. Song, B. S. Kang, S. M. Hwang, 2002, "Finite element analysis of multi-stage deep drawing process for high-precision rectangular case with extreme aspect ratio", *J. Mater. Process. Technol.* Vol 130–131, pp. 128–134.

[6] J. P. Fan, C. Y. Tang, C. P. Tsui, L. C. Chan, T. C. Lee, 2006, "3D finite element simulation of deep drawing with damage development", *International Journal of Machine Tools & Manufacture*, Vol 46, pp. 1035–1044.

[7] CINDAS/USAF CRDA Handbooks Operation Purdue University, "Aerospace Structural Metals Handbook", 1997, Vol 3.

[8] S. Kobayashi, T. Altan. "Metal forming and the finite element method". New York: Oxford University Press; 1989.

[9] ASM International, "Atlas of Stress-Strain Curves", USA, Ohio, 2002, p. 299.

[10] D. F. Eary, E. A. Reed. 1958, "Techniques of Press-working Sheet Metal", 2nd edition. New Jersey: Prentice Hall, Englewood Cliffs. P. 156.